

## The Detection Efficiency of 16-ary QAM

By V. K. PRABHU

(Manuscript received September 6, 1979)

*Efficient use of the radio spectrum is becoming increasingly important since terrestrial and satellite communication needs have placed an increasing burden on the available RF bands. In this paper we determine the detection efficiency of QAM when it is corrupted by Gaussian noise and one or more constant-envelope or amplitude-modulated cochannel interferers. Since the exact method we present involves the summation of an infinite series, upper and lower bounds, which are exponential functions and which are tight for high SNR, are given. Error probability and detection efficiency for 16-ary QAM, 8- and 16-PSK have been evaluated and compared. Cochannel interference immunity of 16-QAM is inferior to that of 8-PSK, but superior to that of 16-PSK.*

### I. INTRODUCTION

In addition to spectrum efficient angle modulation techniques such as PSK, digital radio transmission may use quadrature amplitude shift keying (QASK, also called digital QAM) or combined amplitude and phase shift keying (CAPSK) when these techniques have bandwidth efficiencies of 3 bits/s/Hz or higher. Because of the relative simplicity of implementation and because of superior immunity to Gaussian noise, QAM and especially 16-ary QAM appears more attractive than 16-ary PSK for obtaining high bandwidth efficiencies.

The detection efficiency of QAM in a Gaussian noise channel has been determined in Ref. 1. The method of determining the degradation in detection efficiency caused by bandlimiting and the resultant intersymbol interference appears in Refs. 2 and 3.

However, since attenuation caused by rain may exceed 10 dB per kilometer at 10 GHz or higher carrier frequencies, repeater spacing must be small and cochannel interference may be the major source of impairment if low noise receivers are used in the system. Hence, it is desirable to compare the cochannel interference immunity of QAM to other modulation systems.

We present an analysis to determine the detection efficiency of QAM subject to cochannel interference. We consider both constant-envelope and amplitude-modulated interference and assume the sample-and-detect receivers are used. A correlation receiver, which is optimum for a white Gaussian noise channel, is a specific case of sample-and-detect receiver obtained by choosing an appropriate sampling time and optimum noise bandwidth. In our analysis, we assume that only cochannel interference and thermal noise cause degradation in the system. For the QAM system, we assume coherent demodulation and perfect carrier recovery. Since we are primarily interested in the effect of cochannel interference, we also assume zero intersymbol and other interference.

## II. QAM WITH COCHANNEL INTERFERENCE

The signal space diagram for an  $M$ -ary QAM system appears in Fig. 1. We can write the signal  $s(t)$  as

$$s(t) = \sum_{k=-\infty}^{\infty} \alpha_k \text{rect}\left(\frac{t - kT}{T}\right) \cos(2\pi f_c t) + \sum_{l=-\infty}^{\infty} \beta_l \text{rect}\left(\frac{t - lT}{T}\right) \sin(2\pi f_c t), \quad (1)$$

where  $f_c$  is the carrier frequency,  $T$  the signaling interval, and  $\text{rect}(\cdot)$  the rectangular window function. The two independent and identically distributed digital streams  $\{\alpha_k\}$  and  $\{\beta_l\}$  modulate the envelopes of a cosine and a sine wave and assume values from the set  $\Lambda = \{\pm d, \pm 3d, \dots, \pm(2N-1)d\}$ ,  $M = (2N)^2$ ,  $N$  an integer. Assuming that members of the set  $\Lambda$  occur with equal probability, the peak power in  $s(t)$  is

$$P_{\text{peak}} = \frac{d^2}{T} (2N-1)^2; \quad (2)$$

and the average power

$$P_{\text{av}} = \frac{d^2}{T} \frac{4N^2 - 1}{3}. \quad (3)$$

If the additive zero-mean thermal noise  $n(t)$  with symmetrical double-sided spectral density  $N_0$  around the carrier frequency corrupts  $s(t)$ , the signal after coherent demodulation with a perfect carrier can be written as

$$y_c(t) = \sum_{k=-\infty}^{\infty} \alpha_k \text{rect}\left(\frac{t - kT}{T}\right) + n_c(t) \quad (4)$$

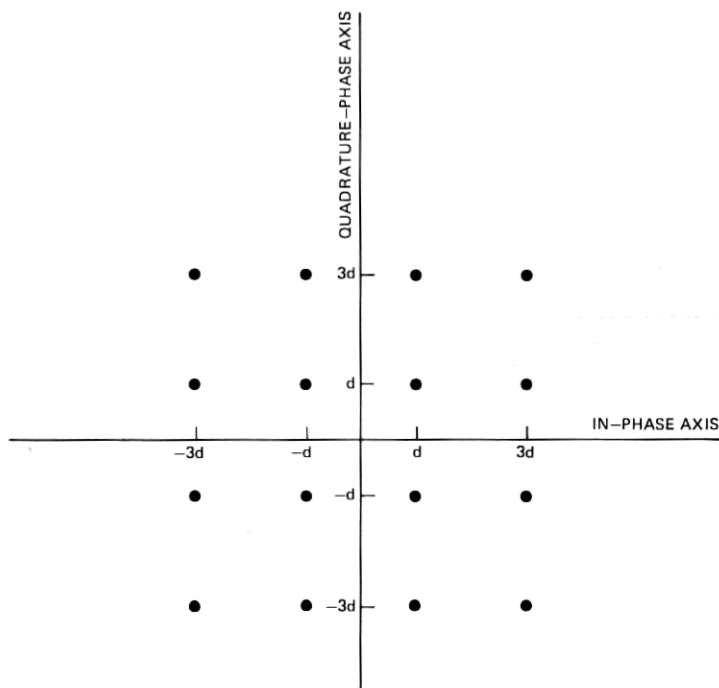


Fig. 1—Signal space diagram for 16-QAM. The minimum distance between any two signal points is  $2d$ , and the symbols on each of the orthogonal carriers take the values  $(\pm d, \pm 3d)$ . The average power on each of the carriers is  $\frac{1}{2}(d^2/T)[(4N^2 - 1)/3]$ , and peak power  $(d^2/T)(2N - 1)^2$ ,  $N = 2$ . The total average power is  $(d^2/T)[(4N^2 - 1)/3]$ .

for the in-phase cosine channel, and

$$y_s(t) = \sum_{l=-\infty}^{\infty} \beta_l \text{rect}\left(\frac{t - lT}{T}\right) + n_s(t) \quad (5)$$

for the quadrature-phase sine channel. In (4) and (5),  $n_c$  and  $n_s$  are identically distributed zero mean Gaussian random variables with the same variance as  $n(t)$ . The random processes  $n_c$  and  $n_s$  occupy bandwidth  $W$  if the bandwidth occupancy of  $n(t)$  is  $2W$  and they have the double-sided spectral density  $2N_0$ .

### 2.1 QAM with constant-envelope cochannel interference

If the cochannel interference consists of one or more statistically independent constant-envelope sinusoidal interferers, the total received signal

$$r(t) = s(t) + \sum_{m=1}^K R_m \cos[2\pi f_c t + \phi_m(t) + \theta_m] + n(t), \quad (6)$$

where  $R_m^2/2$  is the power in the  $m$ th interferer,  $\phi(t)$  the angle modulation that may be present, and  $\theta_m$  a random phase angle. Since we only consider cochannel interference, the modulation  $\phi_m(t)$  is such that all the interferers are within the passband of the receiver. If different sources contribute to the interference, the  $K$  carrier frequencies are not often identical and the carrier phases not truly coherent. Hence, we assume that  $\theta_m$ 's are statistically independent and that they are identically and uniformly distributed over the range  $(-\pi, \pi]$ .

Since the performance of in- and quadrature-phase channels is identical for perfect transmit filters, we shall only consider the cosine channel. After coherent demodulation with a perfectly recovered carrier, the received signal

$$y_c(t) = \sum_{k=-\infty}^{\infty} \alpha_k \text{rect}\left(\frac{t - kT}{T}\right) + \sum_{m=1}^K R_m \cos[\phi_m(t) + \theta_m] + n_c(t). \quad (7)$$

If a sample-and-detect receiver detects the signal, the overall symbol error probability  $P_e$  for the cosine and sine channels is

$$P_e = 2 \left(1 - \frac{1}{2N}\right) \Pr[n_c + \eta > d], \quad (8)$$

where

$$\eta = \sum_{m=1}^K R_m \cos[\phi_m(t) + \theta_m]. \quad (9)$$

References 4 and 5 show that

$$\begin{aligned} \Pr[n_c + \eta > d] &\triangleq P_d = \frac{1}{2} \left\langle \text{erfc} \left[ \frac{d - \eta}{\sigma\sqrt{2}} \right] \right\rangle \\ &= \frac{1}{2} \text{erfc} \left[ \frac{d}{\sigma\sqrt{2}} \right] + \frac{1}{\sqrt{\pi}} \exp\left(-\frac{d^2}{2\sigma^2}\right) \sum_{l=1}^{\infty} H_{2l-1} \left( \frac{d}{\sigma\sqrt{2}} \right) \left( \frac{d^2}{2\sigma^2} \right)^l \frac{\mu_{2l}}{(2l)!} \end{aligned} \quad (10)$$

where

$$\text{erfc}(x) = \frac{2}{\sqrt{\pi}} \int_x^{\infty} e^{-t^2} dt, \quad (11)$$

$\sigma^2$  is the noise power,  $H_k(\cdot)$  the Hermite polynomial of order  $k$ , and  $\mu_{2l}$  the  $2l$ th moment of  $\eta$ . The series in (10) converges absolutely, and a recursive method to calculate moments  $\mu_{2l}$  appears in Ref. 5. After determining  $\mu_{2l}$  from this method,  $P_d$  and  $P_e$  can be calculated with any specified accuracy.

However, for large signal-to-noise ratios (small  $\sigma$  for a given  $d$  and  $N$ ), and for moderately large interference, the series in (10) converges

slowly and we may have to sum an inordinately large number of terms to compute  $P_e$  even with 5 or 10 percent accuracy. Since our main interest lies in performance of QAM for large signal-to-noise ratios (SNR), we prefer to use the simple bounds of Ref. 6, which are tight for high SNR.

If we let

$$P_d = \Pr[n_c + \eta > d], \quad (12)$$

Ref. 6 shows that

$$\begin{aligned} Q_u &= \frac{1}{\sqrt{2\pi}\beta\sigma} \exp(-\beta d + \beta^2\sigma^2/2) \Lambda_\eta(\beta) \geq P_d \geq Q_l \\ &= Q_u \left[ \frac{2}{\sqrt{1+4/(\beta\sigma)^2+1}} - \beta^2 A_2 \frac{\sqrt{1+4/(\beta\sigma)^2}-1}{\sqrt{1+4/(\beta\sigma)^2+1}} - \frac{2}{\sqrt{2\pi}} \frac{1}{\beta\sigma} \right], \quad (13) \end{aligned}$$

where

$$A_2 = \frac{1}{2} \sum_{m=1}^K R_m \frac{I_0^2(\beta R_m) - [I_0(\beta R_m)I_1(\beta R_m)/\beta R_m] - I_1^2(\beta R_m)}{I_0^2(\beta R_m)}, \quad (15)$$

the parameter  $\beta$ ,  $0 < \beta \leq d/\sigma^2$ , the unique solution of

$$d = \beta\sigma^2 + \sum_{m=1}^K R_m \frac{I_1(\beta R_m)}{I_0(\beta R_m)}, \quad (16)$$

and  $I_n(\cdot)$  is the  $n$ th order modified Bessel function of the first kind. If we approximate  $P_d$  by

$$Q_d = \frac{Q_u + Q_l}{2}, \quad (17)$$

the fractional error

$$\begin{aligned} \Delta_d &= \frac{|Q_d - P_d|}{P_d} \leq \frac{1}{2} \frac{Q_u - Q_l}{Q_l}, \quad Q_l > 0 \\ &= \frac{1}{2} \frac{(\sqrt{1+4/(\beta\sigma)^2}-1)(1+\beta^2 A_2) + 2/\sqrt{2\pi}\beta\sigma(\sqrt{1+4/(\beta\sigma)^2+1})}{2 - \beta^2 A_2(\sqrt{1+4/(\beta\sigma)^2}-1) - 2/\sqrt{2\pi}\beta\sigma(\sqrt{1+4/(\beta\sigma)^2+1})}. \quad (18) \end{aligned}$$

We can compute  $\beta$  from the recursive algorithm of Ref. 6, and the value  $Q_d$  from (17) and (13) to (15). If the fractional error  $\Delta_d$  exceeds specified limits, eq. (10) and methods of Ref. 4 can be used to compute  $P_d$ .

### 2.1.1 A simple upper bound on error rate

In this section, we give a simple upper bound on  $P_d$ . This upper bound is similar to the Chernoff bound discussed in Refs. 7 and 8, and can be useful in preliminary system design.

Since

$$I_0(x) \leq e^{x^2/4}, \quad (19)$$

and

$$I_0(x) \leq \exp(|x|), \quad (20)$$

$$\Lambda_\eta(\beta) \leq \exp\left[\beta \sum_{m \in z} R_m + \frac{\beta^2}{4} \sum_{m \in z_c} R_m^2\right], \quad (21)$$

where  $z$  is a subset of  $\{1, 2, \dots, K\}$ , and  $z_c$  denotes the complement of  $z$ . Because

$$P_d \leq \frac{1}{\sqrt{2\pi}\beta\sigma} \exp(-\beta d + \beta^2\sigma^2/2)\Lambda_\eta(\beta), \quad \beta > 0, \quad (22)$$

eqs. (21) and (22) yield

$$P_d \leq \frac{1}{\sqrt{2\pi} \left( \left( d - \sum_{m \in z} R_m \right) / \left( \sigma^2 + \frac{1}{2} \sum_{m \in z_c} R_m^2 \right) \right) \sigma} \cdot \exp\left[ - \left( d - \sum_{m \in z} R_m \right)^2 / \left( \sigma^2 + \frac{1}{2} \sum_{m \in z_c} R_m^2 \right) \right], \quad d - \sum_{m \in z} R_m > 0. \quad (23)$$

Reference 7 gives a method to choose the subset  $z$  so that the upper bound in (23) is minimum.

### 2.1.2 Evaluation of error rate and detection efficiency of 16-ary QAM

For radio system applications, interference immunity of 16-ary ( $2N = 4$ ) QAM is very much of interest. For this system and a single cochannel interferer ( $K = 1$ ), we have calculated the error rate

$$P_e = 2 \left( 1 - \frac{1}{2N} \right) P_d \quad (24)$$

by approximating  $P_d$  by  $Q_d$ . The results are plotted in Fig. 2. For the signal-to-noise and signal-to-interference ratios considered in Fig. 2, the error in the approximation is less than 5 percent. The signal-to-interference ratio (SIR) is the ratio of the average power in the QAM signal to the average power in the interference.

Since a system designer often wants to maintain a specified error rate even when there is interference, the increase in SNR required to maintain three different error rates is plotted in Fig. 3. So that we can compare, in a single ( $K = 1$ ) cochannel interference environment, the detection efficiency of 16-QAM to that of 8- and 16-PSK, we plot the performance results for PSK in Figs. 4 and 5. The signal space diagrams for 8- and 16-PSK are shown in Fig. 6.

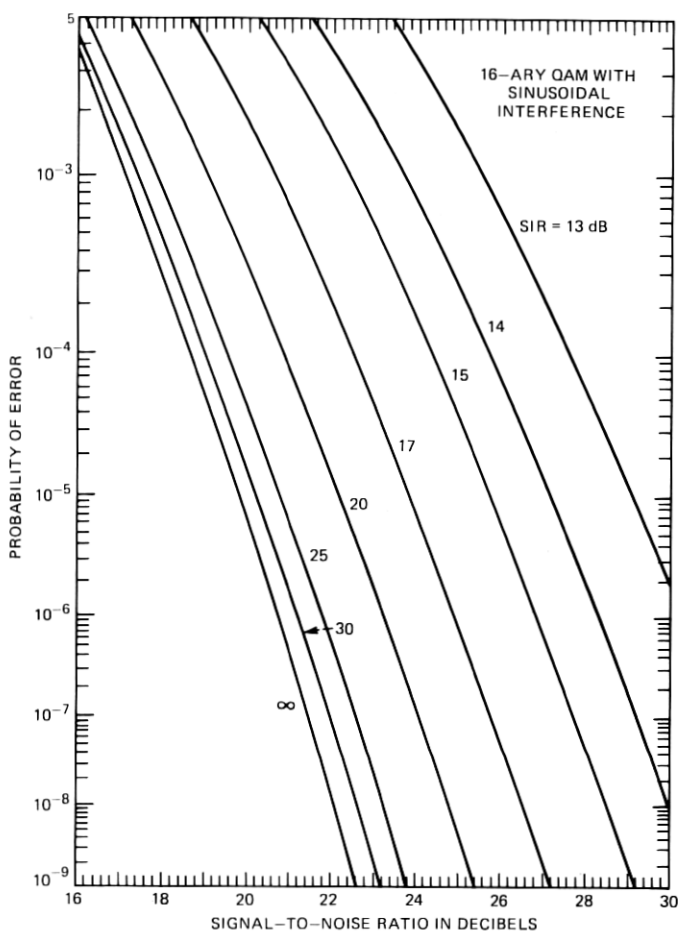


Fig. 2—Error probability for 16-QAM with single constant-envelope cochannel interference. The parameter SNR represents the ratio of total average power in the QAM signal to the noise power. The quantity SIR is the ratio of average signal power to the average power in the interference.

## 2.2 QAM with cochannel amplitude-modulated interference

If the cochannel interference corrupting  $s(t)$  is a set of similar but statistically independent QAM signals, the total received signal

$$r(t) = s(t) + \sum_{m=1}^K R_m \left\{ \sum_{k=-\infty}^{\infty} \alpha_{mk} \text{rect}\left(\frac{t - kT - \tau_m}{T}\right) \cos[2\pi f_c t + \theta_m] + \sum_{l=-\infty}^{\infty} \beta_{ml} \text{rect}\left(\frac{t - lT - \tau_m}{T}\right) \sin[2\pi f_c t + \theta_m] \right\} + n(t), \quad (25)$$

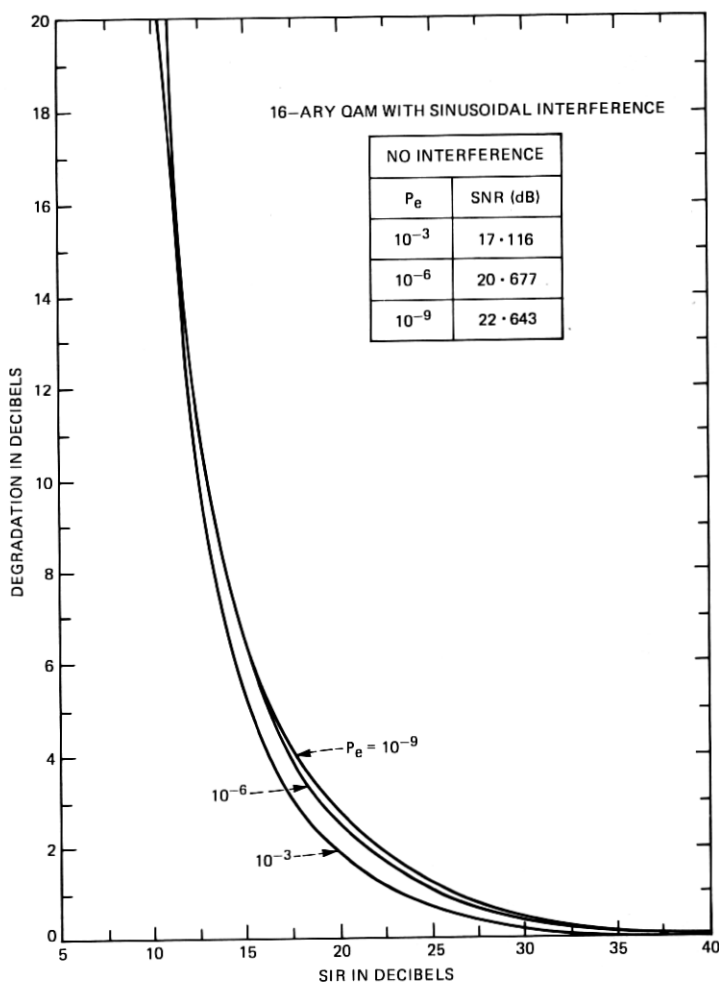


Fig. 3—Degradation in 16-QAM for a single constant-envelope cochannel interference. The ordinate represents the increase in SNR needed to maintain a specified error rate. SNR and SIR are as in Fig. 2.

where two independent and identically distributed digital streams  $\{\alpha_{km}\}$  and  $\{\beta_{kl}\}$  modulate the envelopes of a cosine and a sine wave of the  $m$ th interferer,  $1/R_m^2$ , the signal-to-interference ratio, and  $\tau_m$ , the difference in symbol timing between the desired signal and the  $m$ th interferer. Parameter  $\theta_m$  is a random phase angle and we assume that  $\theta_m$ 's are statistically independent and are identically and uniformly distributed over the range  $(-\pi, \pi]$ . Since the modulation characteristics of the interferer agree with those of the signal,  $\{\alpha_{mk}\}$  and  $\{\beta_{ml}\}$  take values from the set  $\Lambda = \{\pm d, \pm 3d, \dots, \pm(2N-1)d\}$  with equal probability.



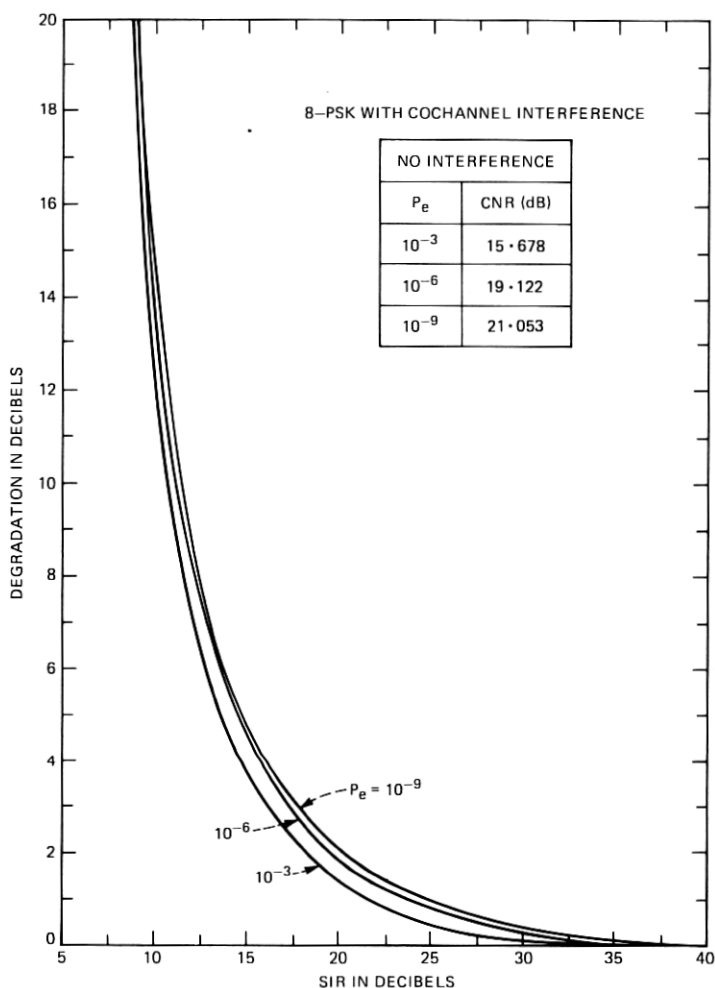


Fig. 4—Degradation in 8-PSK for a single angle-modulated cochannel interference. The ordinate represents the increase in SNR needed to maintain a specified error rate. The SNR is the ratio of average power in the PSK signal to the Gaussian noise power. The quantity SIR is obtained by dividing the average power in the signal by the average power in the interferer.

After coherent demodulation with a perfectly recovered carrier, the received signal on the in-phase channel is

$$y_c(t) = \sum_{k=-\infty}^{\infty} \alpha_k \text{rect}\left(\frac{t - kT}{T}\right) + \sum_{m=1}^K R_m \left\{ \sum_{k=-\infty}^{\infty} \alpha_{mk} \text{rect}\left(\frac{t - kT - \tau_m}{T}\right) \cdot \cos \theta_m + \sum_{l=-\infty}^{\infty} \beta_{ml} \text{rect}\left(\frac{t - lT - \tau_m}{T}\right) \sin \theta_m \right\} + n_c(t). \quad (26)$$

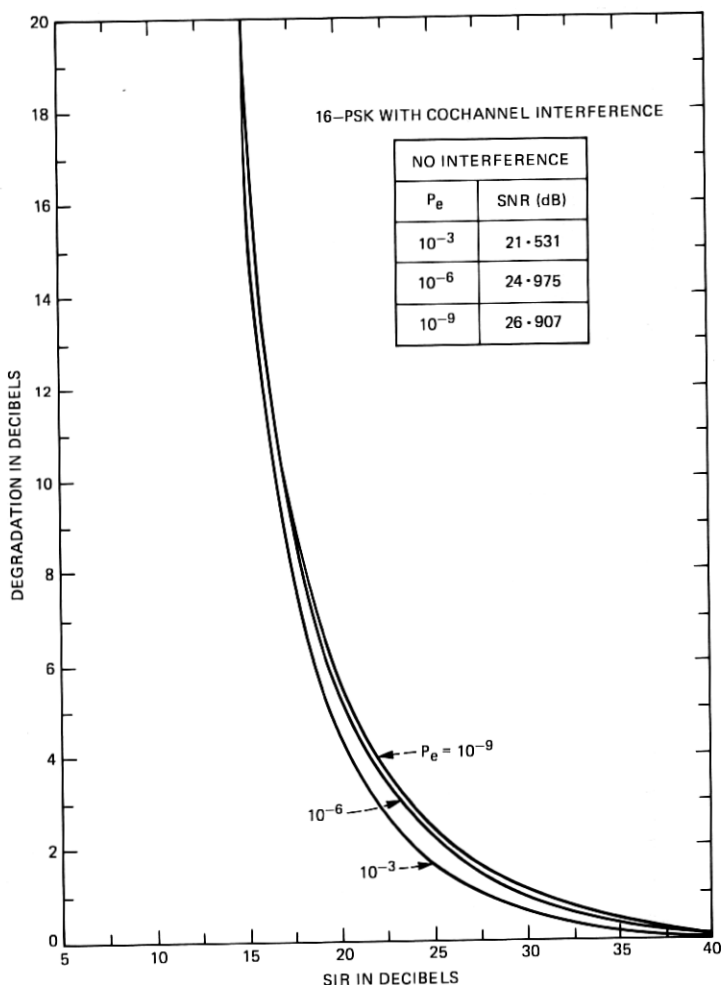


Fig. 5—Degradation in 16-PSK for a single angle-modulated cochannel interference. The ordinate represents the increase in SNR needed to maintain a specified error rate. SNR and SIR are as in Fig. 4.

Rewriting (26),

$$y_c(t) = \sum_{k=-\infty}^{\infty} \alpha_k \text{rect}\left(\frac{t - kT}{T}\right) + \sum_{m=1}^K R_m \sum_{i=-\infty}^{\infty} \sqrt{\alpha_{mi}^2 + \beta_{mi}^2} \cdot \text{rect}\left(\frac{t - iT - \tau_m}{T}\right) \cos(\phi_{mi} + \theta_m) + n_c(t), \quad (27)$$

where

$$\phi_{mi} = -\tan^{-1} \frac{\beta_{mi}}{\alpha_{mi}}. \quad (28)$$

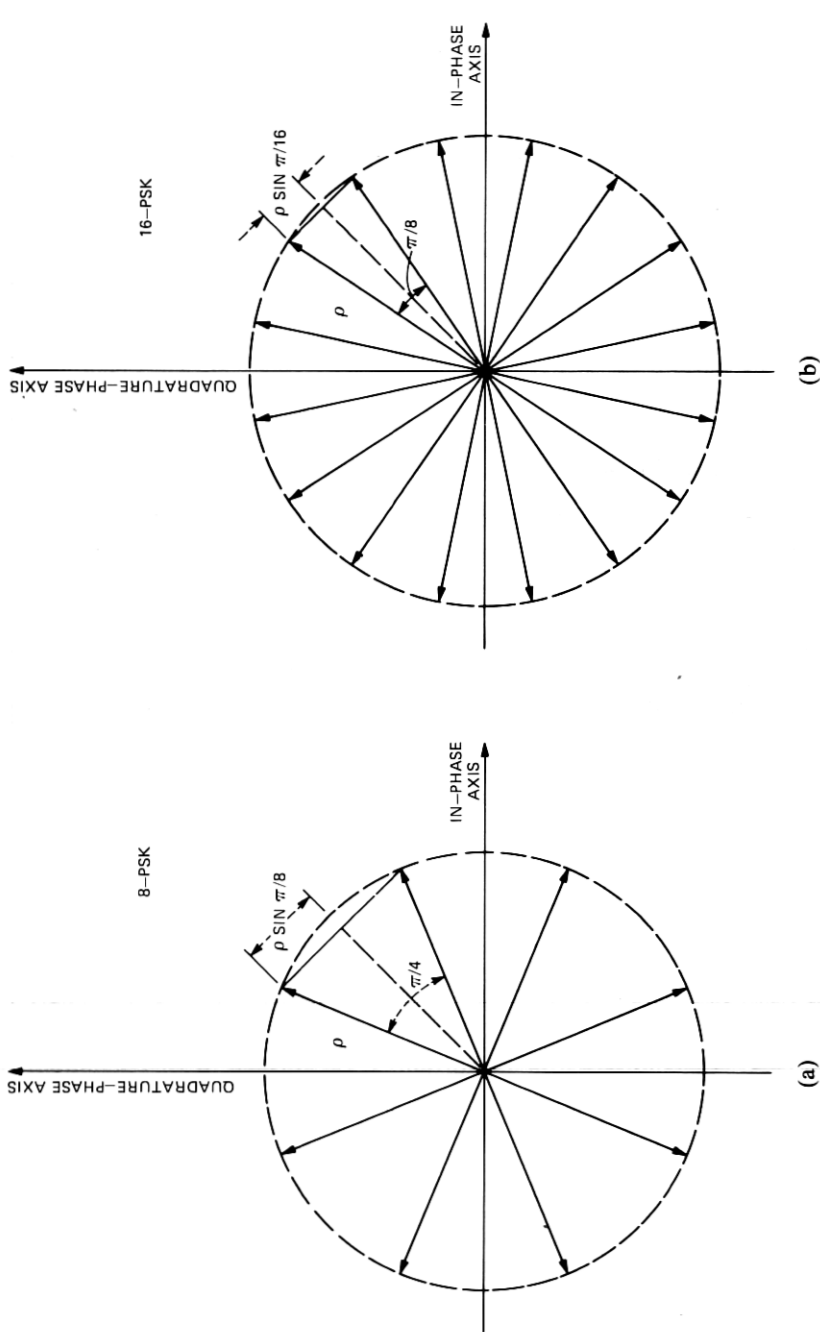


Fig. 6—(a) Signal space diagram for 8-PSK. The length of the signal phasor is represented by  $\rho$ , and  $\rho \sin(\pi/M)$ ,  $M = 8$ , the minimum half-distance between any two signal points. (b) Signal space diagram for 16-PSK. The length of the signal phasor is represented by  $\rho$ , and  $\rho \sin(\pi/M)$ ,  $M = 16$ , the minimum half-distance between any two signal points.

Assuming that  $\tau_m$ 's are statistically independent and that they are identically and uniformly distributed over the range  $[0, T)$ , we can show that the probability of symbol error

$$P_e = 2 \left[ 1 - \frac{1}{2N} \right] P_d, \quad (29)$$

where

$$P_d = \frac{1}{(2N)^2} \sum_{k=1}^{(2N)^2} \Pr[n_c + \eta_k > d], \quad (30)$$

where

$$\eta_k = \sum_{m=1}^K R_m d\mu_k \cos(\theta_m) \quad (31)$$

$$\mu_k = \sqrt{p_k^2 + q_k^2}, \quad p_k, q_k \in \{1, 3, \dots, (2N-1)\}. \quad (32)$$

We note from (30) and (12) that the error probability of QAM with modulated cochannel interference is the mean of error probabilities of  $[(2N)^2]^K$  QAM systems with different but constant envelope cochannel interference. Hence, we can determine (30) by evaluating or bounding each of the terms by the methods of Section 2.1.

For a 16-ary QAM system and a single cochannel 16-ary QAM interferer, we have calculated the error probability with a 5-percent accuracy. The results are shown in Fig. 7. The increase in SNR required to maintain three different error rates is plotted in Fig. 8. Note that the average power in the  $m$ th interferer is

$$P_{\text{av}_m} = R_m^2 \frac{d^2}{T} \frac{4N^2 - 1}{3}, \quad (33)$$

and its peak power

$$P_{\text{peak}_m} = R_m^2 \frac{d^2}{T} (2N - 1)^2. \quad (34)$$

Also, we can compare the performance of 16-QAM with cochannel modulated interference to that of 8- and 16-PSK by using the results of Figs. 4 and 5.

### III. DISCUSSION OF PERFORMANCE OF 16-QAM

Comparing Figs. 3 and 8, we note that the amplitude-modulated single cochannel interference produces more degradation in 16-QAM than constant-envelope interference of the same average power. If  $I^2/2$  is the average power in the interferer, the peak value for the constant-envelope interferer is  $I$ ; for a modulated interferer, it is

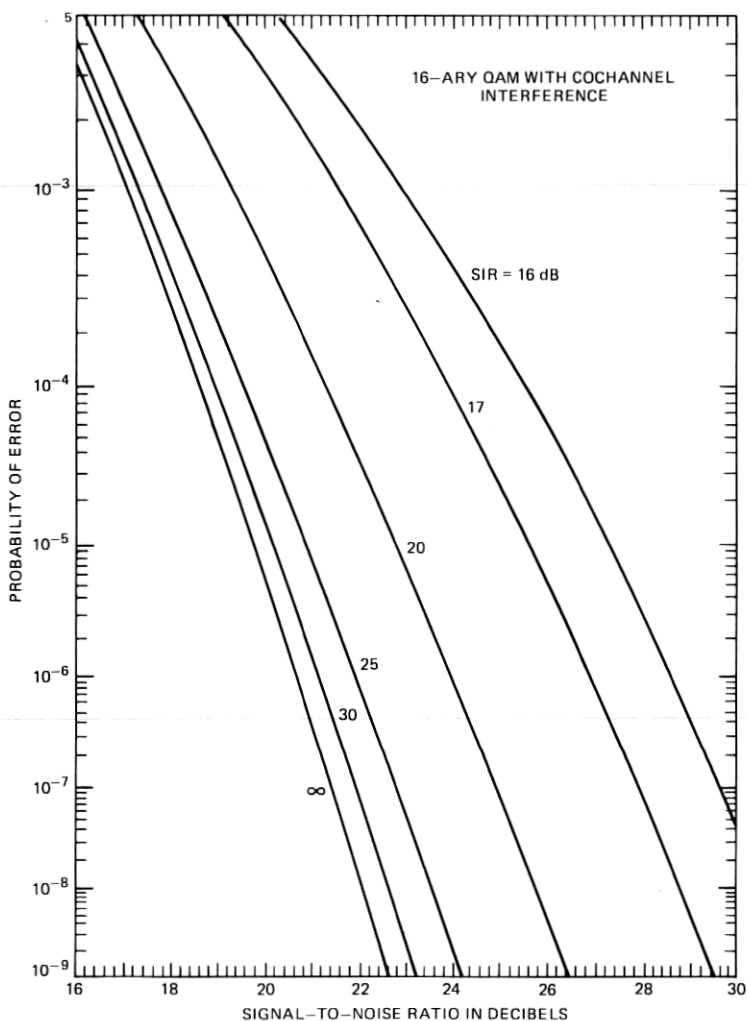


Fig. 7—Error probability for 16-QAM with single 16-QAM cochannel interference. The parameter SNR represents the ratio of total average power in the QAM signal to the Gaussian noise power. The quantity SIR is the ratio of total average signal power to the total average power in the interference.

$I(2N - 1)(3/4N^2 - 1)^{1/2}$ . Hence, the peak amplitude for a modulated interference is  $3/\sqrt{5}$  times the peak amplitude for a constant-envelope interference of the same power. As shown in Fig. 9, the minimum half-distance between any two signal points is reduced by the peak amplitude of the cochannel interference. Since the probability of error is a strong function of this minimum half-distance, the degradation in 16-QAM with modulated interference is higher than with constant-envelope interference.

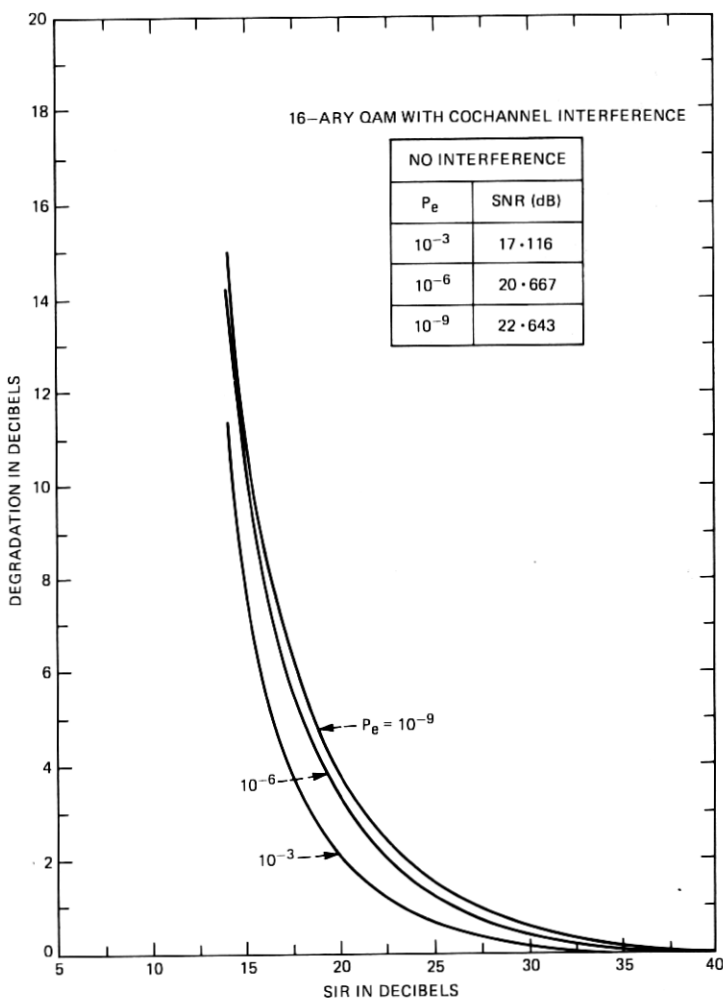


Fig. 8—Degradation in 16-QAM for a single 16-QAM cochannel interference. The ordinate represents the increase in SNR needed to maintain a specified error rate. SNR and SIR are as in Fig. 7.

If we compare the detection efficiency of 16-QAM to that of 8-PSK by using Figs. 4 and 8, we observe that 8-PSK is superior to 16-QAM. For example, for an error rate of  $10^{-6}$  and signal-to-modulated interference ratio of 15 dB, QAM suffers a degradation of 10.3 dB in SNR; for the same parameters, the degradation in 8-PSK is 4.5 dB. For an SIR of 30 dB, these degradations are 0.5 dB for QAM and 0.3 dB for PSK.

If we now consider the performance of 16-PSK (see Fig. 5), it is inferior to that of 16-QAM. For an error rate of  $10^{-6}$  and an SIR of

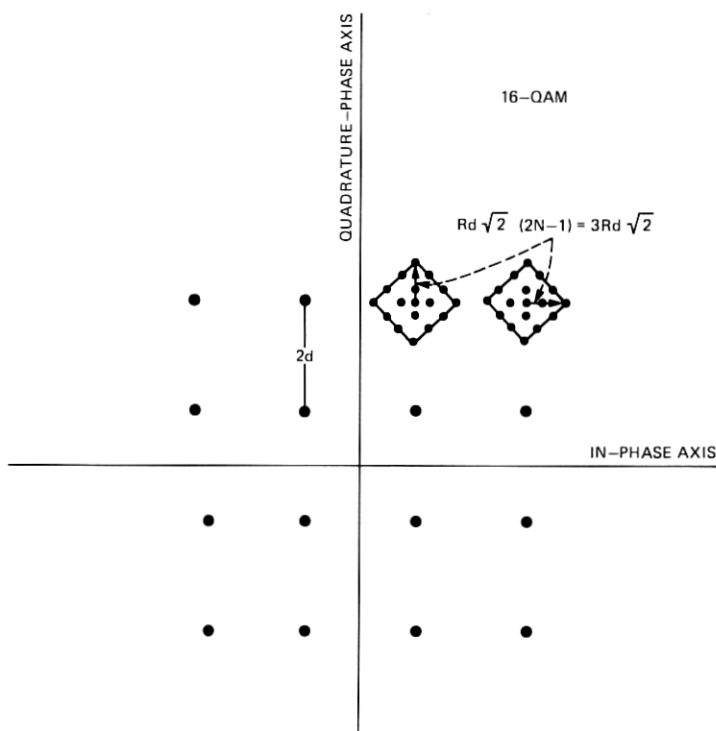


Fig. 9—Signal space diagram for 16-QAM with single 16-QAM cochannel interference. If  $2d$  represents the minimum distance between any two  $(2N)^2$ -QAM,  $N = 2$ , signal points and if the ratio of the average power in the QAM interferer to the average signal power is  $R^2$ , the maximum value of the interference is  $Rd\sqrt{2}(2N - 1)$ .

15 dB, the degradation in 16-PSK is 19.6 dB; for an SIR of 30 dB, it is 0.9 dB.

The inferior performance of 16-PSK and superior performance of 8-PSK can be explained by using the signal space diagrams of 16-QAM in Fig. 9 and 8- and 16-PSK in Figs. 10 and 11. For an  $M$ -ary PSK of signal amplitude  $\rho$  and interference  $\rho R$ , the minimum half-distance between signal points becomes  $\rho \sin(\pi/M)$  without interference and  $\rho \sin(\pi/M) - \rho R$  with interference. The parameter  $R^2$  represents the ratio of interference power to signal power. Since the degradation in SNR is a strong function of the proportional decrease in minimum half-distance, this degradation is a strong function of  $R/\sin(\pi/M)$ . As noted before, this proportional decrease for  $(2N)^2$ -QAM with modulated interference is  $R(2N - 1)$ . For 16-ary QAM, this proportional decrease becomes  $3R$ ; for 8-PSK,  $2.61R$ , for 16-PSK  $5.13R$ . Therefore, 16-QAM performs poorer than 8-PSK and better than 16-PSK.

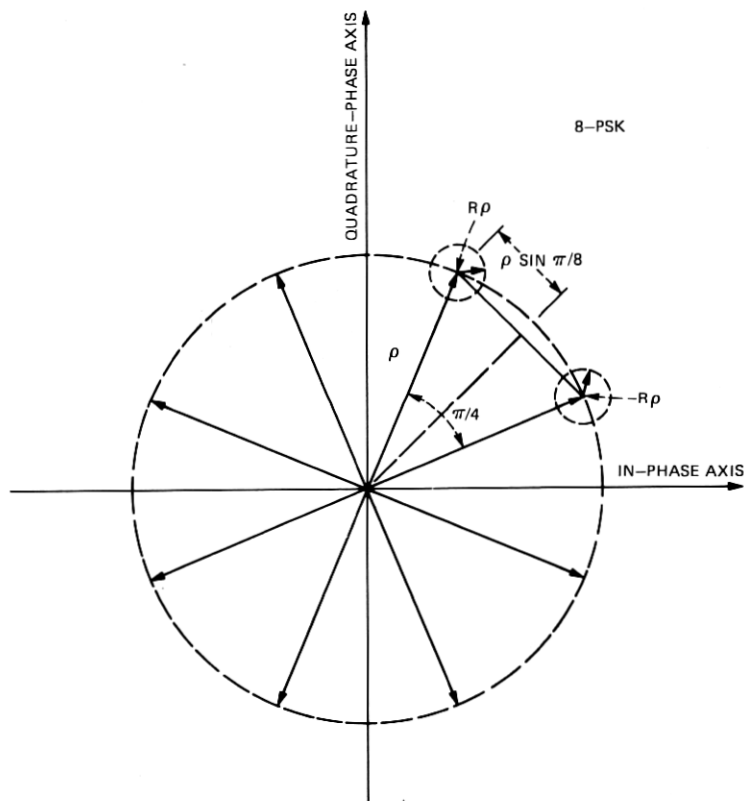


Fig. 10—Signal space diagram for 8-PSK with a single angle-modulated cochannel interference. If  $\rho$  represents the length of the signal phasor and  $R$  the ratio of the length of the interference phasor to that of the signal, the maximum value of the interference is  $\rho R$ .

For a 16-ary QAM system, we can determine, by using methods given in this paper, the degradation produced by cochannel interference. We can compare this degradation to that in  $M$ -ary PSK so that we are aware of comparative advantages of different modulation techniques in our system design. For some typical error rates and SIR, we give the signal-to-noise ratio required by different systems in Table I.

#### IV. SUMMARY AND CONCLUSIONS

We determine the detection efficiency of 16-ary QAM so that it can be compared to 8- and 16-PSK.

We give a method to determine the error probability of QAM when it is corrupted by Gaussian noise and one or more constant-envelope or amplitude-modulated cochannel interferers. Since the method in-



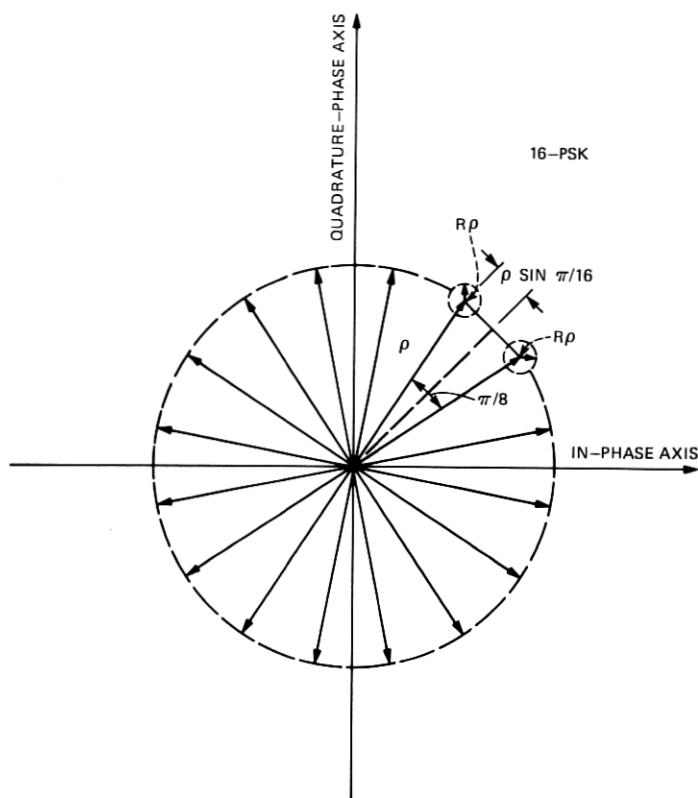


Fig. 11—Signal space diagram for 16-PSK with a single angle-modulated cochannel interference. If  $\rho$  represents the length of the signal phasor and  $R$  the ratio of the length of the interference phasor to that of the signal, the maximum value of the interference is  $\rho R$ .

volves the summation of an infinite series, simple upper and lower bounds, which are tight for high SNR, are given.

Error probability and detection efficiency of 16-ary QAM, 8- and 16-PSK have been evaluated and compared. The cochannel interference immunity of 16-QAM is inferior to that of 8-PSK, but superior to that of 16-PSK. Detailed comparisons can be found in Figs. 3, 4, 5, and 8 and Table I.

Table I—Comparison of modulated cochannel interference immunity of QAM to that of PSK

	For Zero Interference, SNR (in dB) for an Error Rate of		For an SIR (in dB) of							
	$10^{-3}$	$10^{-6}$	30		25		20		15	
			Increase in SNR (in dB) to	Increase in SNR (in dB) to	Increase in SNR (in dB) to	Increase in SNR (in dB) to	Increase in SNR (in dB) to	Increase in SNR (in dB) to	Increase in SNR (in dB) to	Increase in SNR (in dB) to
			$10^{-3}$	$10^{-6}$	$10^{-3}$	$10^{-6}$	$10^{-3}$	$10^{-6}$	$10^{-3}$	$10^{-6}$
8-PSK	15.68	19.12	0.16	0.31	0.48	0.80	1.37	1.90	3.73	4.52
16-QAM	17.12	20.68	0.22	0.45	0.69	1.24	2.14	3.31	7.85	10.33
16-PSK	21.53	24.98	0.57	0.93	1.62	2.20	4.44	5.29	17.99	19.61

## V. ACKNOWLEDGMENT

Inquiries from W. T. Barnett prompted this investigation. We are grateful to him for bringing this problem to our attention and for his advice and encouragement.

## REFERENCES

1. R. W. Lucky, J. Salz, and E. J. Weldon, Jr., *Principles of Data Communication*, New York: McGraw-Hill, 1968, pp. 177-195.
2. C. M. Thomas, "Final Report on Amplitude-Phase Keying Techniques," TRW Technical Report, August 1971.
3. M. Araki, Y. Saito, and I. Horikawa, "Application of the Series Expansion Method to Error Rate Calculation in Multilevel QAM System," *IECE Japan, J61-B* (Nov. 1978), pp. 970-971.
4. V. K. Prabhu, "Error Rate Considerations for Coherent Phase-Shift Keyed Systems with Cochannal Interference," *BSTJ.*, 48, No. 3 (March 1969), pp. 743-767.
5. V. K. Prabhu, "Some Considerations of Error Bounds in Digital Systems," *BSTJ.*, 50, No. 10 (Dec. 1971), pp. 3127-3151.
6. V. K. Prabhu, "Modified Chernoff Bounds for PAM Systems with Noise and Interference," unpublished work.
7. V. K. Prabhu, "Error-Probability Upper Bound for Coherently Detected psk Signals with Cochannal Interference," *Electronics Letters*, Vol. 5, August 1969.
8. A. Javed and R. P. Tetarenko, "Error Probability Upper Bound for Coherently Detected QASK Signals with Cochannal Interference," *IEEE Trans. Commun., COM-27*, No. 12 (December 1979), pp. 1782-1785.